Decoding the X-Ray Flare from MAXI J0709–159 Using Optical Spectroscopy and Multiepoch Photometry

Suman Bhattacharyya[1] [iD], Blesson Mathew[1] [iD], Savithri H Ezhikode[1] [iD], S. Muneer[2] [iD], Selvakumar G.[2], Maheswer G.[2], R. Arun[1,2] [iD], Hema Anilkumar[1], Gourav Banerjee[1] [iD], Pramod Kumar S[2], Sreeja S Kartha[1] [iD], KT Paul[1], and C. Velu[2]

[1] Department of Physics and Electronics, CHRIST (Deemed to be University), Hosur Main Road, Bangalore, India
[2] Indian Institute of Astrophysics, Koramangala, Bangalore, India
Received 2022 March 15; revised 2022 June 5; accepted 2022 June 9; published 2022 July 11

Abstract

We present a follow-up study on the recent detection of two X-ray flaring events by MAXI/Gas Slit Camera observations in soft and hard X-rays from MAXI J0709–159 in the direction of HD 54786 (LY CMa), on 2022 January 25. The X-ray luminosity during the flare was around 10^{37} erg s^{-1} (MAXI), which got reduced to 10^{32} erg s^{-1} (NuSTAR) after the flare. We took low-resolution spectra of HD 54786 from the 2.01 m Himalayan Chandra Telescope and the 2.34 m Vainu Bappu Telescope (VBT) facilities in India, on 2022 February 1 and 2. In addition to Hα emission, we found emission lines of He I in the optical spectrum of this star. By comparing our spectrum of the object with those from the literature we found that He I lines show variability. Using photometric studies we estimate that the star has an effective temperature of 20,000 K. Although HD 54786 is reported as a supergiant in previous studies, our analysis favors it to be evolving off the main sequence in the color–magnitude diagram. We could not detect any infrared excess, ruling out the possibility of IR emission from a dusty circumstellar disk. Our present study suggests that HD 54786 is a Be/X-ray binary system with a compact object companion, possibly a neutron star.

1. Introduction

Be/X-ray binaries (BeXRBs) form a major subclass of high-mass X-ray binaries that consist of a Be star and a compact object (e.g., Rappaport & van den Heuvel 1982; Reig 2011). The compact object accretes matter from the decretion disk of the Be star. The possible compact objects are neutron stars (NSs; Okazaki & Negueruela 2001), white dwarfs (WDs; Kennea et al. 2021), and black holes (BHs; Casares et al. 2014), yet NSs are the most frequently observed companion than other kinds (Belczynski & Ziolkowski 2009). BeXRBs can be persistent or transient in nature. Whereas in the latter case it exhibits outburst events, which are classified as Type I, where X-ray luminosity $L_x \leqslant 10^{37}$ erg s^{-1} and occurs regularly, separated by the orbital period, and Type II, where $L_x \geqslant 10^{37}$ erg s^{-1}, these outbursts are less frequent and are not modulated on the orbital period (Stella et al. 1986). The transient X-ray behavior is caused by the interaction of the compact object with the material in the circumstellar disk (Monageng et al. 2017; Okazaki & Negueruela 2001). A Be star is a special class of massive B-type main-sequence (MS) star, surrounded by a geometrically thin, equatorial, gaseous, decretion disk (Meilland et al. 2007). Be stars are primarily identified by means of a Hα emission feature formed in the ionized decretion disk of Be stars, by means of the recombination process (e.g., Banerjee et al. 2021; Mathew et al. 2012).

Recently, on 2022 January 25 at 10:42:28 UT, the Monitor of All-sky X-ray Image (MAXI) Gas Slit Camera (GSC)

(Negoro et al. 2016) nova alert system triggered a bright uncatalogued X-ray transient source with an X-ray flux of 266 ± 32 mCrab over the scan. The source of flare is situated at an R.A. of 107°280 and decl. of −15°923. The intensity of the X-ray flux was comparatively low before (09:09 UT) and after (12:15 UT) the event (Serino et al. 2022). The source was named MAXI J0709–159. Following that, at 13:44 UT (on the same day), the Neutron Star Interior Composition Explorer Mission (NICER; Gendreau et al. 2016) reported X-ray emission from the position of R.A. = 107°392 and decl. = −16°108, with an X-ray flux of 10 mCrab in the energy band of 0.2−12 keV (Iwakiri et al. 2022).

Kobayashi et al. (2022) found that the position of the Be star HD 54786 matches with that of the region from where X-ray emission is detected by NICER. Based on the GSC energy spectrum study, they suggested HD 54786 to be a companion of MAXI J0709–159, and that the system might be a supergiant fast X-ray transient (SFXT) or a Cir X-1–type object. This was further corroborated from the study of Negoro et al. (2022), who analyzed the X-ray emission using the Nuclear Spectroscopic Telescope Array (NuSTAR; Harrison et al. 2013) observations from 00:21 to 11:21 UT on 2022 January 29.

The first spectroscopic study of HD 54786 is by Merrill & Burwell (1949), who identified hydrogen emission lines in the spectrum. Morgan et al. (1955) classified this star as a blue supergiant with luminosity class I. Subsequently, it was listed in the Be star catalog of Jaschek & Egret (1982). Later, Chojnowski et al. (2015) also identified this star as a Be star. Houk & Smith-Moore (1988) estimated its spectral type to be B1/B2.

This Letter follows up on the recent X-ray flaring event of HD 54786, combining optical spectroscopy and photometry

Table 1
Observation Log of HD 54786 from HCT and VBT

Star Name	Date and Time (UT) of Observation (yyyy-mm-dd, hh:mm)	HJD	R.A.	Decl.	Exposure Time (s)
HCT Observation					
HD 54786	2022-02-01, 16:22	2459611	07 09 36.97	−16 05 46.1	240
	2022-02-02, 13:39	2459612	⋯	⋯	180
VBT Observation					
HD 54786	2022-02-01, 16:00	2459611	07 10 46.97	−16 07 46.1	1800
	2022-02-02, 15:08	2459612	⋯	⋯	2400

over various epochs, to better understand the nature of the prospective BeXRB system.

2. Observations

2.1. Optical Spectroscopy

We collected two low-resolution spectra of HD 54786, from the HFOSC instrument mounted on the 2.01 m Himalayan Chandra Telescope (HCT)[3] located at Hanle, Ladakh, India. We observed the star on two consecutive dates, 2022 February 1 and 2. The spectral coverage is from 5500 to 8800 Å, where both the red region spectra are obtained with grism 8 (5800–8300 Å) and a 167 μm slit, providing an effective resolution of 7 Å at Hα.

To validate the spectra obtained from HCT, we acquired two additional simultaneous low-resolution spectra at the same epochs from the opto mechanics research (OMR) instrument, mounted on the 2.34 m reflecting telescope situated at the Vainu Bappu Observatory (VBO), Kavalur, Tamil Nadu, India. In VBT the photographic sensor employed is an Andor CMOS high speed read out sensor, comprising 1024×256 pixels having a pixel size of 26 μm. The spectra are obtained in the wavelength region of 5500−8500 Å, at settings particularly centered at the Hα line with a resolving power of 1000. Table 1 presents the observation log of HD 54786 from HCT and VBT facilities.

For both observations, dome flats taken with halogen lamps were utilized for flat-fielding the images. Bias subtraction, flat-fielding, and spectrum extraction were performed using IRAF routines. The wavelength-calibrated spectra are continuum fitted using IRAF tasks. Additionally, the resulting spectra from VBT are further normalized using a python routine.

2.2. Gaia Astrometric Data

The astrometric data of HD 54786 are taken from the latest data release of Gaia (Gaia EDR3; Gaia Collaboration et al. 2021). The geometrical distance estimates by Bailer-Jones et al. (2021) are used in this study. The color–magnitude diagram (CMD) analysis using the Gaia EDR3 data has given our work greater context (Section 3.2).

2.3. X-Ray

HD 54786 has been continuously monitored with MAXI for years. As the recent MAXI archival data were not available, we used the publicly available processed GSC (2−30 keV) light curves (version 7Lrkn 4h), which is frequently updated every

4 hr. NuSTAR also observed the source during the quiescent period for 18 ks on 2022 January 29. The two coaligned focal plane modules, FPMA and FPMB, detected hard X-ray photons (3−79 keV) from the source. We generated the spectra and light curves from FPMA and FPMB observations using standard pipelines in the NuSTAR Data Analysis Software (NUSTARDAS V2.0.0; CALDB Version 20220131). The source spectra were extracted for circular regions of radii 32."32, while the background spectra were generated for annular regions ($r_{in} = 32.32''$, $r_{out} = 60''00$) centered on the source.

## 3. Results

3.1. Gaia EDR3 Analysis

The distance of HD 54786 was reported to be different in previous studies. So we used the Gaia EDR3 distance estimate of 2955^{+244}_{-175} pc (Bailer-Jones et al. 2021) for further analysis.

From the Gaia database and the field image of 2MASS (Figure 1), we note that there is another star (source B) at a separation of 6."5 in the southwest direction of HD 54786. This is not prominent in the optical image (e.g., SDSS9) but is detectable in 2MASS J, H, and K_S composite images. The astrometric parameters such as parallax and proper motions of two stars must be similar and within uncertainty limits for being considered to be in a binary system (Arun et al. 2021a). We found that the distances of the two sources are matching within uncertainties. However, their proper motion values are considerably different. Hence, for the present study we will not consider them as associated and further discussion will purely be on HD 54786.

3.2. Gaia CMD Analysis

HD 54786 is reported as a supergiant by Houk & Smith-Moore (1988), belonging to the luminosity class Ib. We constructed the Gaia CMD for this star to identify its location. Considering its Gaia EDR3 distance and A_V value of 0.93 (as estimated from Green's map; Green et al. 2019), we plotted the corresponding M_G versus $G_{(BP-RP)0}$ CMD for the star. Additionally, we overplotted the probability distribution (Gaussian fitted at three contour levels) of previously studied B-type stars (Huang et al. 2010), Be stars (Bhattacharyya et al. 2021, and references therein), giant stars (Hohle et al. 2010), and supergiants (Georgy et al. 2021) to better understand the location of HD 54786. From Pecaut & Mamajek (2013), the zero-age main sequence (ZAMS) line does not extend beyond B9 spectral type in M_G and $G_{(BP-RP)0}$ values. Hence, we utilized the closely matching 60 Myr isochrone track from Modules for Experiments in Stellar Astrophysics (MESA)

---

[3] http://www.iiap.res.in/iao/hfosc.html
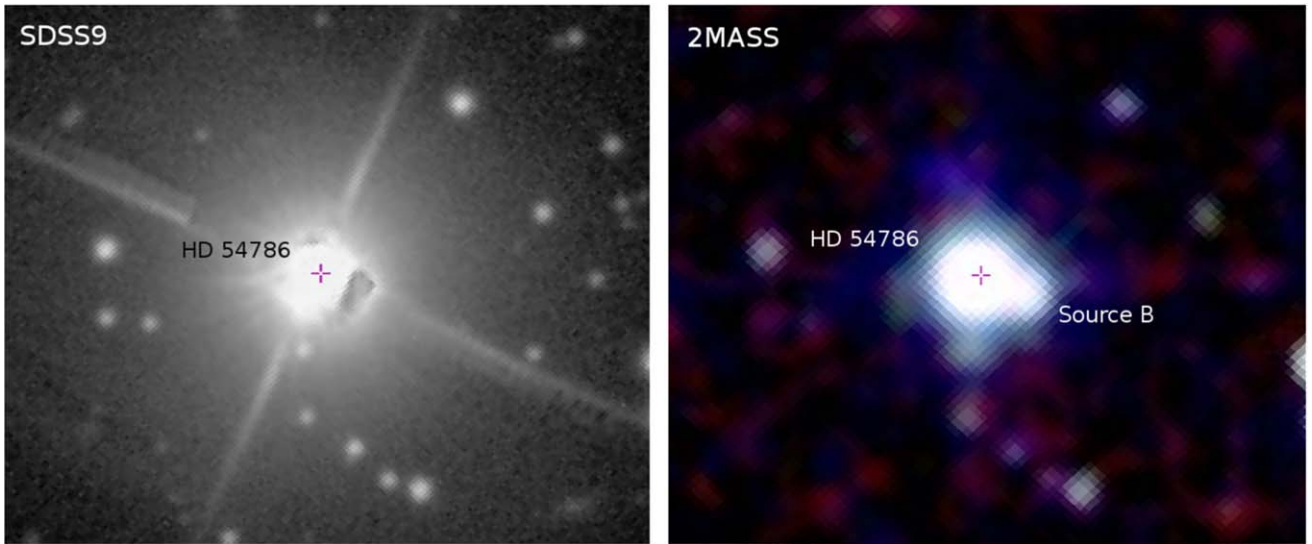
Figure 1. Images of the region around HD 54786 (FoV 1'.3) from the SDSS9 survey (left) in gray scale and the 2MASS survey (right) in J, H, and K_S color composites, respectively. The source B is distinguishable in the 2MASS image but not in the SDSS9 image.
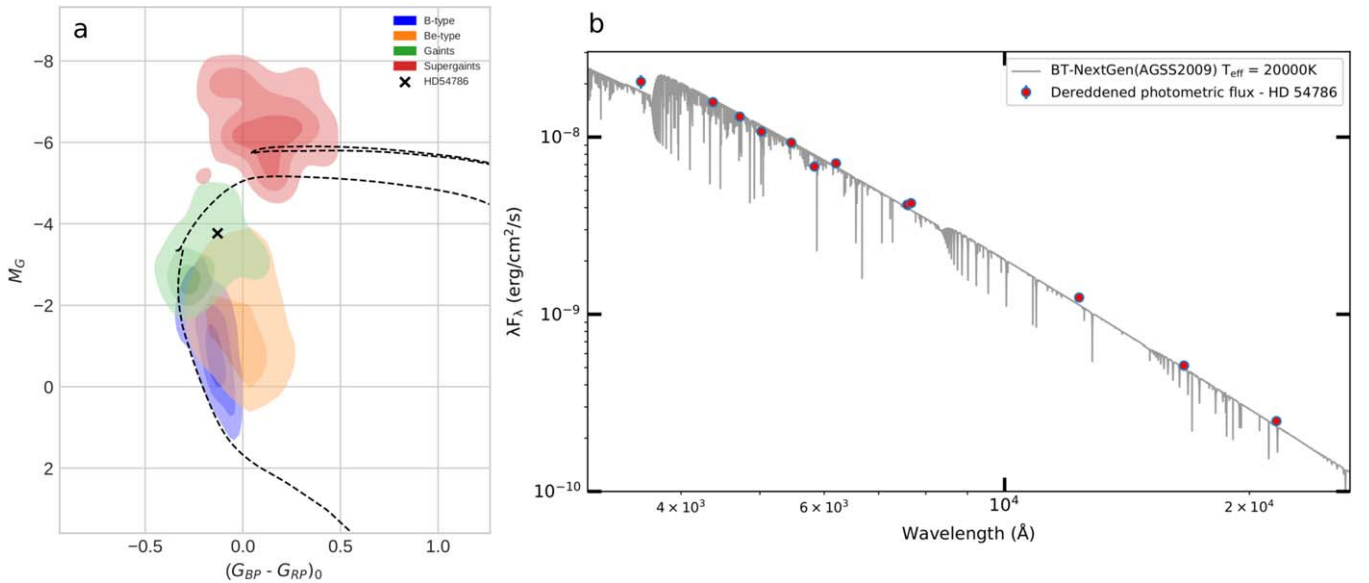

Figure 2. (a) The Gaia CMD of HD 54786 having absolute Gaia G and color-corrected (BP–RP) magnitudes available from Gaia Collaboration et al. (2021). The probability distribution (Gaussian fitted at three contour levels) of the B, Be stars, giants, and supergiants are shown in blue, orange, green, and red shaded colors, respectively. The black dashed line in the plot represents the isochrone of 60 Myr with $V/V_{crit} = 0.4$ and $[Fe/H] = 0$. (The top black dashed line is the blue loop part of the same isochrone.) (b) In the SED, the flux values of the star HD 54786 are fitted with the theoretical BT-NextGEN(ASGG2009) model at $T_{eff} = 20{,}000$ K and $\log(g) = 3$, using the chi-squared minimization method.

Isochrones and Evolutionary Tracks (MIST) (Choi et al. 2016; Dotter 2016), which is overplotted in the CMD with $V/V_{crit} = 0.4$, since that is the only model available in the MIST database for a rotating system. Moreover, we adopted the metallicity value of $[Fe/H] = 0$, corresponding to solar metallicity $Z_\odot = 0.0142$ (Asplund et al. 2009) for the tracks. The CMD showing the location of HD 54786, with the representative locations of MS B-type stars, Be stars, giants, and supergiants are presented in Figure 2(a).

Our analysis shows that the location of HD 54786 is near to the top of the distribution of B and Be stars. It is also noted that the star resides inside the distribution of giant stars but below that of supergiants. This indicates that HD 54786 might be an evolved star with respect to B/Be types. However, its location also conveys that it is not a supergiant star.

3.3. Spectral Energy Distribution

As a next step, we fitted the spectral energy distribution (SED) for HD 54786 to reestimate its spectral type. For generating the SED, we used the Johnson U magnitude; B, V, g', r', and i' magnitudes from APASS (Henden et al. 2015); G, G_{RP}, and G_{BP} magnitudes from Gaia EDR3; and the infrared J, H, and K_s magnitudes from 2MASS. The SED is generated with the python routine used in Arun et al. (2021b). Figure 2(b) presents the SED plot generated for HD 54786. From a grid of BT-NextGen (AGSS2009; Hauschildt et al. 1999) theoretical stellar atmospheres at solar metallicity and $\log(g) = 3-4$ (since it seems to be evolved from the MS in the CMD), corresponding to various temperatures, we found that the best fit (by means of chi-squared minimization)
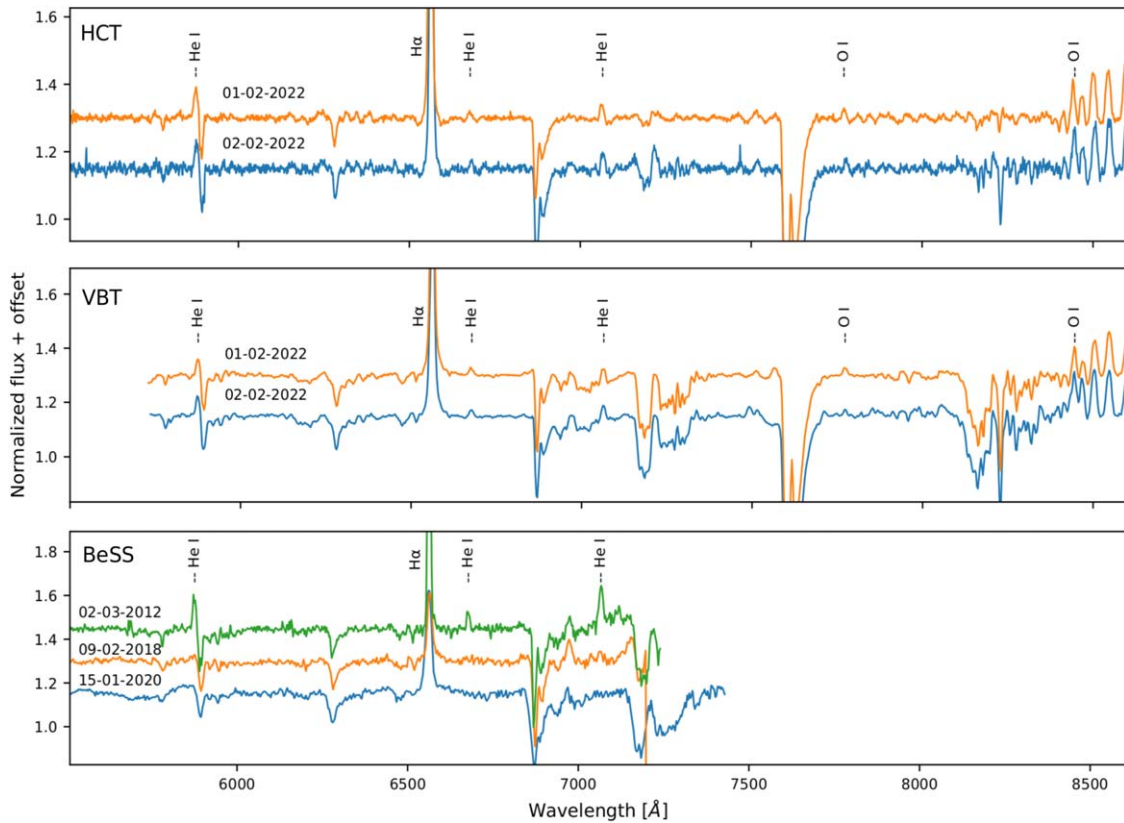
Figure 3. Representative spectra of HD 54786 showing different spectral features in the wavelength range of 5500–8500 Å. The spectra from HCT, VBT, and BeSS spectra are listed in the top, middle, and bottom panels.

corresponds to an effective temperature (T_{eff}) of $20,000 \pm 500$ K with $\log(g)$ of 3.

The obtained T_{eff} matches with a spectral type of B2 (Pecaut & Mamajek 2013), if it is an MS star. However, the stellar radius estimated from the SED is $R_*/R_\odot = 11.8$. This value is higher than that of an MS star (5.7 $R_\odot$) with a similar T_{eff} (Pecaut & Mamajek 2013). Cox (2000) reported that a supergiant with a similar spectral type will have a radius of $\sim 19\,R_\odot$. Our estimated $\log(g)$ and stellar radius values suggest that the star is not on the MS phase, but is in the evolved region (off the MS), which is in agreement with our CMD analysis. Hence, we will not resort to identifying any specific spectral type for this star in the present work. Instead, we agree that the spectral type is similar to the previous estimates of B1/B2 (Houk & Smith-Moore 1988), and we will put forth the T_{eff} and $\log(g)$ value as the derivatives from this study.

Furthermore, we do not notice any significant IR excess in the SED, suggesting the absence of dust emission from the circumstellar disk. If the disk contains a dust component, it should appear as flux excess in the 2MASS colors. The lack of a dusty disk eliminates the possibility of the extended accretion disk. However, based on the Hα emission, a decretion disk surrounding the Be star is possible, with the excess caused by free–free emission or thermal bremsstrahlung, which is more apparent in the mid-IR range. Although mid-IR data are available in ALLWISE survey (Cutri et al. 2013), we did not consider it since there is a nearby star that will contaminate the WISE magnitudes.

3.4. Prominent Spectral Features Identified in HD 54786

We then identified all major spectral features observed in the spectra of HD 54786 taken using VBT and HCT. We found

that the Hα line is visible in single-peak emission in all spectra, for each of the epochs. The average signal-to-noise ratio (S/N) of every spectrum taken is greater than 120. In the case of HCT, we detected that Hα equivalent width (EW) was -17.6 Å on 2022 February 1, whereas it was -16.9 Å on 2022 February 2. The Hα EW from HCT spectra decreased by a value of 0.7 Å within 1 day. Figure 5 (top panel) represents the Hα EW variation with time. Apart from Hα, emission lines of He I: 5876, 6678, 7065; O I: 7772, 8446 Å; and P13–P17 of the Paschen series are also noticed on both the dates. In addition, we also observed telluric O_2 absorption bands of 6867 and 7593 Å (Smette et al. 2015) on both the cases. Figure 3 shows the representative spectra of HD 54786 obtained using HCT and VBT.

Interestingly, Hα EW of HD 54786 was found to be -23 Å when observed on 2022 January 28 by Nesci (2022), which was taken 3 days after the X-ray flaring. It is intriguing to notice that the Hα EW was higher on the nights closer to the flaring event and was decreasing to -16.9 Å on 2022 February 2. However, any major change of EW is not noticed for any other emission line feature other than Hα, during the period of our observations.

3.4.1. Spectral Features Observed in Data from the BeSS Database

We queried in the BeSS database (Neiner et al. 2011) to check whether any observation of this star was done by amateur astronomers. We found a total of three spectra for HD 54786 taken by amateur astronomers Dejean Pastor (spectrum taken on 2020 January 15), Cazzato (2018 February 9), and

Buil (2012 March 2), in the BeSS database. The spectra are represented in Figure 3.

It was found that Hα EW was the maximum (around −28.3 Å) on 2012 March 2. This value decreased to −2.7 Å on 2018 February 9. Interestingly, Hα EW again increased to −12.1 Å on 2020 January 15. Hβ is also seen in emission (EW = −3.1 Å) on 2012 March 2, whereas it shows weak absorption on the other two dates. Moreover, He I 5876, 6678, and 7065 Å lines are noticed in emission only on 2012 March 2, whereas on the other two occasions (2018 February 9 and 2020 January 15, respectively) we are not seeing these three lines in emission.

3.4.2. Variability in He I Emission Lines

Comparing the spectra obtained by us using the HCT facility and those retrieved from the BeSS database, we found a considerable variability exhibited by He I 5876, 6678, and 7065 Å emission lines. All these lines were visible in emission on 2012 March 2 when amateur astronomer Buil observed HD 54786 (C11 LISA ATIK314L+). On the contrary, all were present in absorption in the BeSS spectra on 2018 February 9 and 2020 January 15. However, we found all of them in emission when observed with HCT on 2022 February 1 and 2.

It is known that He I emission lines are found rarely in Be stars (Banerjee et al. 2021) and are produced in high-temperature regions with $T \sim 15,000$ K (Kwan & Fischer 2011). Bahng & Hendry (1975) proposed that these lines may either be a temporary phenomenon or non-LTE effects are responsible for their selective excitation. Since we find that He I lines are showing intensity changes over a short period of time, it may be a temporary phenomenon, as proposed by Bahng & Hendry (1975). Apparao & Tarafdar (1994) proposed that in Be stars, He I emission lines can be produced by the influence of a compact binary companion that is accreting matter from the disk of the primary (here the Be star) star.

The occasional appearance and disappearance of He I emission lines in the series of spectra used in our study indicate that the disk temperature of HD 54786 becomes higher during the flaring event and has a recurring nature. However, the appearance of these lines in emission on 2022 February 1 and 2 hints toward some sudden increase in disk temperature. This can happen if some flare activity takes place from a nearby companion star, which is what has been observed recently in the case of HD 54786. Hence, our study suggests the possibility that X-ray flaring probably resulted in the formation of He I emission lines, which may disappear as time progresses. We did not see such a correlation earlier since X-ray data were not available then. We are doing follow-up observations for HD 54786 to check whether any X-ray flaring event leads to the formation of He I emission lines or not.

3.5. X-Ray Spectral Analysis

We performed the X-ray spectral analysis of the NuSTAR observation of the source for the quiescent period using the X-ray spectral fitting package *Xspec* (version 12.12.0; Arnaud 1996). The spectra were grouped to have a minimum of 15 counts per bin. Above 25 keV, the spectra were dominated by the background. As a result, we looked at the spectra in the 3−25 keV energy range. We used an empirical power-law model modified by galactic absorption to fit the spectra. The galactic absorption was modeled with the neutral
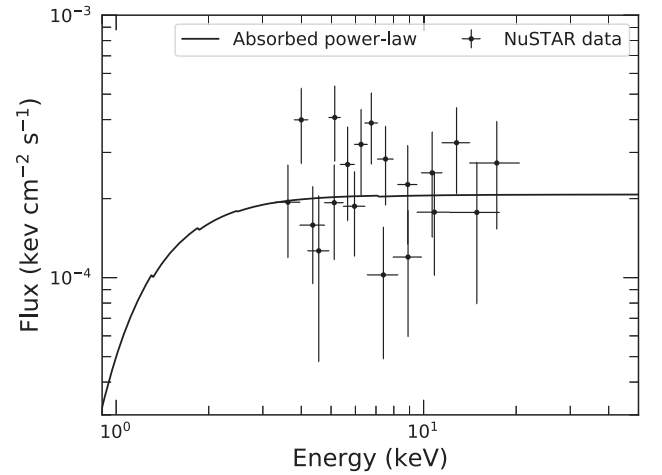
Figure 4. NuSTAR (FPMA and FPMB) spectra modeled with *constant × TBabs × powerlaw* in the 3–25 keV band. The solid line shows the power-law continuum corrected for the Galactic absorption.

hydrogen column density N_H fixed at 5.6×10^{21} cm^{-2}, obtained using the HI4PI survey (HI4PI Collaboration et al. 2016). We did not consider the intrinsic absorption as it was not considerably significant. To account for the cross-normalization disparities between the FPMA and FPMB data, a constant factor ($0.94^{+0.37}_{-0.28}$) was applied. A photon index (slope of the hard X-ray power-law) of $\Gamma = 2.00^{+0.47}_{-0.43}$ was obtained from the model fit with a fit statistic of χ^2(degrees of freedom) = 18.26(16). To measure the unabsorbed flux we added another component *cflux* to the power-law model. We measured the unabsorbed X-ray flux in the energy range of 3−25 keV to be $7.03^{+1.81}_{-1.68} \times 10^{-13}$ erg cm^{-2} s^{-1}. The best-fit model and unfolded spectra are shown in Figure 4.

The X-ray (2–10 keV) flux values of the source for the flaring period are obtained from Kobayashi et al. (2022). We then calculated the luminosity of the two detected peaks during the flaring, which was reported by MAXI/GSC at 10:42 and 13:48 UT on 2022 January 25. The luminosity for the first and second flares are estimated to be $6.42^{+2.82}_{-1.67} \times 10^{36}$ erg s^{-1} and $1.67^{+4.29}_{-1.05} \times 10^{37}$ erg s^{-1}, respectively. Moreover, we calculated the unabsorbed 2–10 keV flux from the NuSTAR data from 00:21 to 11:21 UT on 2022 January 29, about 4 days after the initial MAXI detection. The spectral fit is found to be $5.33^{+1.47}_{-1.32} \times 10^{-13}$ erg cm^{-2} s^{-1} and the X-ray luminosity, for a distance of 2955 pc, to be $5.57^{+1.54}_{-1.38} \times 10^{32}$ erg s^{-1}.

3.6. Is HD 54786 a γ Cas Variable or a BeXRB?

Based on irregular photometric variability, HD 54786 is reported as a γ Cas variable (Alfonso-Garzón et al. 2012). However, it is difficult to differentiate γ Cas variables and BeXRBs based on optical variability alone. They can differ significantly depending on their X-ray characteristics (Reig 2011). In this section we evaluate whether HD 54786 is a γ Cas variable or a BeXRB binary system.

Typically, γ Cas variables (mostly a Be + white dwarf system) show harder X-ray spectra, best fit with a thin plasma emission model (Smith et al. 2016). On the contrary, a power-law model is usually observed in high-mass X-ray binaries (HMXBs), where BeXRB is a subclass. Moreover, γ Cas variables do not exhibit large X-ray outbursts (Reig 2011). The hard X-ray emission from BeXRBs are usually nonthermal in
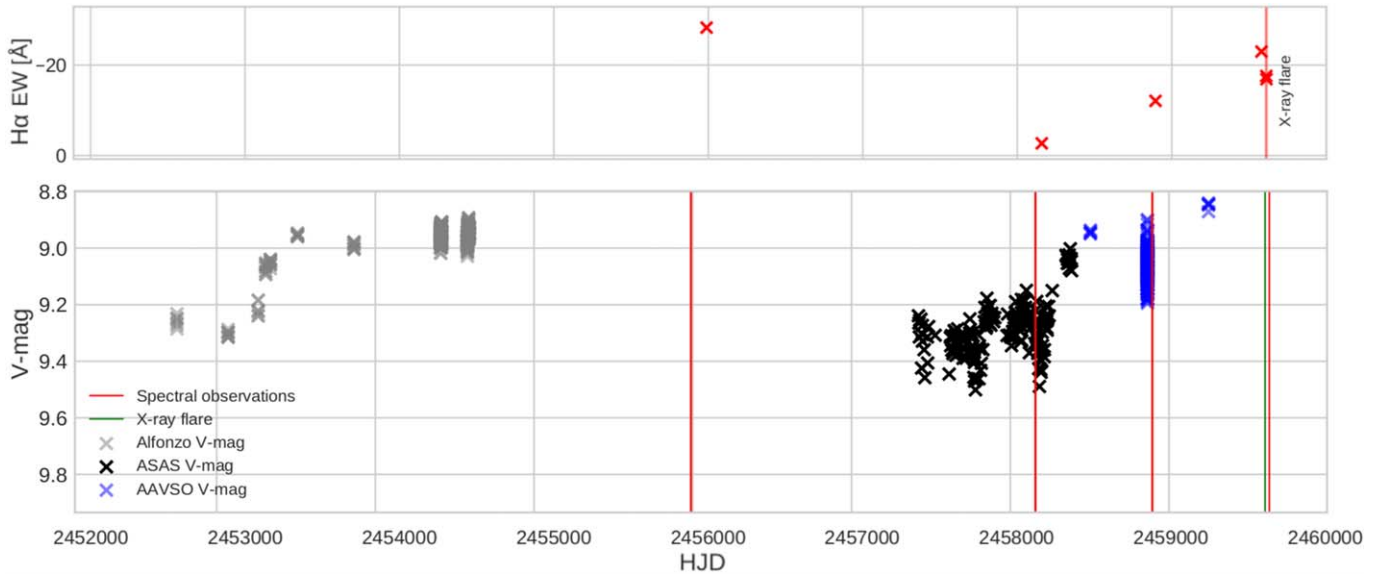
Figure 5. Variation of Hα EW and *V* magnitude shown by HD 54786. In the top panel, the red crosses represent the Hα EW. In the bottom panel, the gray, black, and blue crosses show *V*-magnitude values obtained from Alfonso-Garzón et al. (2012), ASAS, and AAVSO, respectively. The vertical red lines and green line represent the time of spectral observations and the X-ray flaring event, respectively. It is noticed that its *V* magnitude steadily increases over the span of observations. The epoch of BeSS spectra from 2018 February (HJD 2458150) and the photometry measurements from ASAS are seen to overlap in the figure. During that time, the Hα EW was significantly lower (-2.7 Å), with an average *V* magnitude of 9.2−9.3. Again from 2018 May−September (HJD 2,458,239 to 2,458,362), *V*-magnitude values were between 9.0 and 9.1. Then, a considerable rise in Hα EW (to -12.1 Å) in the BeSS spectra of 2020 January (HJD 2,458,849) was detected, whereas the AAVSO *V*-magnitude value was found to range between 8.9 and 9.2. Subsequently, the *V* magnitude changed to 8.85 during AAVSO observations in 2021 February (HJD 2,459,246). However, a considerable variability of Hα EW is seen, i.e., from -23.2 to -16.9 Å, if we compare our observations with that of Nesci (2022).

nature, which is not the case in γ Cas variables (Kubo et al. 1998).

For HD 54786, the X-ray luminosity of the source was found to be of the order 10^{37} erg s^{-1}, when observed by MAXI/GSC on two different times on the same date, i.e., on 2022 January 25. The luminosity then dropped to 10^{32} erg s^{-1} on 2022 January 29, when observed by NuSTAR. The X-ray flare of such a scale suggests that HD 54786 belongs to the class of BeXRB, where the companion is a compact object, possibly a neutron star (e.g., Reig 2011; Okazaki & Negueruela 2001). The X-ray luminosity as estimated by us implies that the outburst is of Type I (Stella et al. 1986). However, further study using time period analysis and periodic pulsations will be necessary to confirm this.

4. Discussion

Our study suggests that HD 54786 might be an evolved Be star rather than an MS star or a supergiant. Using SED analysis we estimated its $T_{\rm eff}$, log(g), and radius ($R_*/R_\odot$) values to be 20,000 K, 3, and 11.8, respectively. We found a considerable decrease in Hα EW from -23 Å on 2022 January 28 (noticed by Nesci 2022 3 days after the X-ray flare) to -16.9 Å on 2022 February 2. It is interesting to notice that the Hα EW was higher on the nights closer to the flaring event and decreased on later dates. The variability we observed in He I 5876, 6678, and 7065 Å emission lines indicate that the disk temperature of HD 54786 becomes higher during the flaring event and has a recurring nature.

Our results further suggest the possibility that X-ray flaring probably resulted in the formation of He I emission lines, which may disappear as time progresses. Moreover, the X-ray analysis points out that the outburst is of Type I and HD 54786 belongs to the class of BeXRB consisting of a compact object companion.

Furthermore, we studied the epoch-wise variation of *V* magnitude and Hα EW seen in HD 54786 in the context of the X-ray flare event. This is done to check whether the variation of *V* magnitude and Hα EW is co-related with the X-ray flaring event or not. For that, we searched the MAXI on-demand webpage for the epochs where a variation in Hα was observed (2012, 2018, and 2020), and did not find any significant X-ray detection during these periods. Also, we compiled the *V*-magnitude values from Alfonso-Garzón et al. (2012) (between 2003 April and 2008 May), ASAS-SN Catalog of Variable Stars III (Shappee et al. 2014; Jayasinghe et al. 2019; 2016 February to 2018 September), and from the AAVSO database (for the period from 2019 January to 2021 February). Figure 5 presents the variation of Hα EW and *V* magnitude shown by HD 54786. Interestingly, our study shows that there was a gradual increase in *V* magnitude, which took place until 2021 February, the last date of observation available before the X-ray flaring event. Further observational data, particularly simultaneous observations, are required to understand whether the *V* magnitude and Hα emission are associated with the X-ray outburst or not. Also, it will help to assess the periodicity of the HD 53786 BeXRB system.

ORCID iDs

Suman Bhattacharyya ⓘ https://orcid.org/0000-0002-1920-6055
Blesson Mathew ⓘ https://orcid.org/0000-0002-7254-191X
Savithri H Ezhikode ⓘ https://orcid.org/0000-0003-1795-3281
S. Muneer ⓘ https://orcid.org/0000-0002-4024-956X
R. Arun ⓘ https://orcid.org/0000-0002-4999-2990
Gourav Banerjee ⓘ https://orcid.org/0000-0001-8873-1171
Sreeja S Kartha ⓘ https://orcid.org/0000-0002-7666-1062

References

Alfonso-Garzón, J., Domingo, A., Mas-Hesse, J. M., & Giménez, A. 2012, A&A, 548, A79
Apparao, K. M. V., & Tarafdar, S. P. 1994, ApJ, 420, 803
Arnaud, K. A. 1996, in ASP Conf. Ser., 101, Astronomical Data Analysis Software and Systems V, ed. G. H. Jacoby & J. Barnes (San Francisco, CA: ASP), 17
Arun, R., Mathew, B., Maheswar, G., et al. 2021b, MNRAS, 507, 267
Arun, R., Mathew, B., Rengaswamy, S., et al. 2021a, MNRAS, 501, 1243
Asplund, M., Grevesse, N., Sauval, A. J., & Scott, P. 2009, ARA&A, 47, 481
Bahng, J. D. R., & Hendry, E. 1975, PASP, 87, 137
Bailer-Jones, C. A. L., Rybizki, J., Fouesneau, M., Demleitner, M., & Andrae, R. 2021, AJ, 161, 147
Banerjee, G., Mathew, B., Paul, K. T., et al. 2021, MNRAS, 500, 3926
Belczynski, K., & Ziolkowski, J. 2009, ApJ, 707, 870
Bhattacharyya, S., Mathew, B., Banerjee, G., et al. 2021, MNRAS, 507, 3660
Casares, J., Negueruela, I., Ribó, M., et al. 2014, Natur, 505, 378
Choi, J., Dotter, A., Conroy, C., et al. 2016, ApJ, 823, 102
Chojnowski, S. D., Whelan, D. G., Wisniewski, J. P., et al. 2015, AJ, 149, 7
Cox, A. N. 2000, Allen's Astrophysical Quantities (New York: Springer)
Cutri, R. M., Wright, E. L., Conrow, T., et al. 2013, yCat, II/328
Dotter, A. 2016, ApJS, 222, 8
Gaia Collaboration, Brown, A. G. A., Vallenari, A., et al. 2021, A&A, 649, A1
Gendreau, K. C., Arzoumanian, Z., Adkins, P. W., et al. 2016, Proc. SPIE, 9905, 99051H
Georgy, C., Saio, H., & Meynet, G. 2021, A&A, 650, A128
Green, G. M., Schlafly, E., Zucker, C., Speagle, J. S., & Finkbeiner, D. 2019, ApJ, 887, 93
Harrison, F. A., Craig, W. W., Christensen, F. E., et al. 2013, ApJ, 770, 103
Hauschildt, P. H., Allard, F., & Baron, E. 1999, ApJ, 512, 377
Henden, A. A., Levine, S., Terrell, D., & Welch, D. L. 2015, AAS Meeting, 225, 336.16
HI4PI Collaboration, Ben Bekhti, N., Flöer, L., et al. 2016, A&A, 594, A116
Hohle, M. M., Neuhäuser, R., & Schutz, B. F. 2010, AN, 331, 349
Houk, N., & Smith-Moore, M. 1988, Michigan Catalogue of Two-dimensional Spectral Types for the HD Stars. Volume 4, Declinations −26°.0 to −12°.0, 4 (Ann Arbor, MI: Univ. of Michigan)
Huang, W., Gies, D. R., & McSwain, M. V. 2010, ApJ, 722, 605
Iwakiri, W., Gendreau, K., Arzoumanian, Z., et al. 2022, ATel, 15181, 1
Jaschek, M., & Egret, D. 1982, IAUS, 98, 261
Jayasinghe, T., Stanek, K. Z., Kochanek, C. S., et al. 2019, MNRAS, 485, 961
Kennea, J. A., Coe, M. J., Evans, P. A., et al. 2021, MNRAS, 508, 781
Kobayashi, K., Negoro, H., Sugita, S., et al. 2022, ATel, 15188, 1
Kubo, S., Murakami, T., Ishida, M., & Corbet, R. H. D. 1998, PASJ, 50, 417
Kwan, J., & Fischer, W. 2011, MNRAS, 411, 2383
Mathew, B., Banerjee, D. P. K., Naik, S., & Ashok, N. M. 2012, MNRAS, 423, 2486
Meilland, A., Stee, P., Vannier, M., et al. 2007, A&A, 464, 59
Merrill, P. W., & Burwell, C. G. 1949, ApJ, 110, 387
Monageng, I. M., McBride, V. A., Coe, M. J., Steele, I. A., & Reig, P. 2017, MNRAS, 464, 572
Morgan, W. W., Code, A. D., & Whitford, A. E. 1955, ApJS, 2, 41
Negoro, H., Kohama, M., Serino, M., et al. 2016, PASJ, 68, S1
Negoro, H., Mihara, T., Pike, S., et al. 2022, ATel, 15193, 1
Neiner, C., de Batz, B., Cochard, F., et al. 2011, AJ, 142, 149
Nesci, R. 2022, ATel, 15194, 1
Okazaki, A. T., & Negueruela, I. 2001, A&A, 377, 161
Pecaut, M. J., & Mamajek, E. E. 2013, ApJS, 208, 9
Rappaport, S., & van den Heuvel, E. P. J. 1982, in Be stars; Proc. of the Symp., 98, ed. M. Jaschek & H. G. Groth (Dordrecht: Reidel), 327
Reig, P. 2011, Ap&SS, 332, 1
Serino, M., Negoro, H., Nakajima, M., et al. 2022, ATel, 15178, 1
Shappee, B. J., Prieto, J. L., Grupe, D., et al. 2014, ApJ, 788, 48
Smette, A., Sana, H., Noll, S., et al. 2015, A&A, 576, A77
Smith, M. A., Lopes de Oliveira, R., & Motch, C. 2016, AdSpR, 58, 782
Stella, L., White, N. E., & Rosner, R. 1986, ApJ, 308, 669